ARTICLES
PUBLISHED ONLINE: 9 JANUARY 2011 | DOI: 10.1038/NCHEM.956
nature chemistry

Cis-dicarbonyl binding at cobalt and iron porphyrins with saddle-shape conformation

Knud Seufert[1], Marie-Laure Bocquet[2], Willi Auwärter[1], Alexander Weber-Bargioni[3], Joachim Reichert[1,3], Nicolás Lorente[4] and Johannes V. Barth[1,3]*

Diatomic molecules attached to complexed iron or cobalt centres are important in many biological processes. In natural systems, metallotetrapyrrole units carry respiratory gases or provide sensing and catalytic functions. Conceiving synthetic model systems strongly helps to determine the pertinent chemical foundations for such processes, with recent work highlighting the importance of the prosthetic groups' conformational flexibility as an intricate variable affecting their functional properties. Here, we present simple model systems to investigate, at the single molecule level, the interaction of carbon monoxide with saddle-shaped iron– and cobalt–porphyrin conformers, which have been stabilized as two-dimensional arrays on well-defined surfaces. Using scanning tunnelling microscopy we identified a novel bonding scheme expressed in tilted monocarbonyl and *cis*-dicarbonyl configurations at the functional metal-macrocycle unit. Modelling with density functional theory revealed that the weakly bonded diatomic carbonyl adduct can effectively bridge specific pyrrole groups with the metal atom as a result of the pronounced saddle-shape conformation of the porphyrin cage.

The interaction of diatomic molecules with complexed transition-metal centres is decisive in many biological processes. Nature notably takes advantage of metalloporphyrins with iron or cobalt centres as prosthetic groups to handle respiratory gases, and sensing and catalytic functions, and a plethora of model systems have been investigated to determine the underlying elementary chemical binding mechanisms[1–3]. In recent years it has become clear that the conformational flexibility of the porphyrin macrocycle sensitively interferes, as a decisive factor, in the regulation of the relevant functional properties[4–10]; however, many questions remain regarding the intricate interplay between structural distortions and the ligation of small adducts. Here we report a molecular-level investigation on the interaction of carbon monoxide with simple iron and cobalt tetraphenyl-porphyrin model systems, adopting a distinct saddle-shape conformation, one of the prominent nonplanar macrocycle geometries, following adsorption on a smooth metal surface[11,12]. Our scanning tunnelling microscopy (STM) and molecular manipulation experiments revealed a surprising carbonyl binding scheme that contrasts with the common wisdom of exclusive axial monocarbonyl ligation at biological or related synthetic porphyrin species. Density functional theory (DFT) calculations for both adsorbed and isolated cobalt tetraphenyl-porphyrin demonstrate that CO can in fact bridge specific pyrrole groups with the metal centre; this effect is induced by the saddle-shape conformation and explains the observed mono- and *cis*-dicarbonyl geometries. Our findings suggest a novel ligation scheme for CO at metalloporphyrins that requires consideration regarding its potential influence on the groups' functionality.

Despite the many studies focusing on the binding mechanism of diatomic molecules at the haem prosthetic group[13] and the related relevance of CO as a cellular signalling molecule[14,15], the factors regulating the affinity and geometry of CO remain to be fully elucidated. In the context of discrimination between CO of endogenous origin and from dioxygen, many explanations invoke the local environment of the prosthetic group as acting specifically on the ligated molecules via steric, hydrogen-bonding or electrostatic interactions[1,16–18]. During analysis it is generally assumed that monocarbonyl axial ligation takes place right at the metal centre[1], and distortions of the functional group may occur in the presence of the adduct. This calls for investigations that directly probe the interaction of CO with model porphyrin systems, where the conformation of the macrocycle is controlled and a surrounding is provided that precludes the interference of additional protein or other units. We realized such an elementary arrangement by confining cobalt– and iron–tetraphenyl-porphyrin (CoTPP, FeTPP) on well-defined Cu(111) and Ag(111) surfaces. Through surface anchoring, arrays of coordinatively unsaturated species can be generated with a known macrocycle conformation[11,12], allowing their response upon exposure to CO to be investigated *in situ* using STM.

Identification of CO ligation mode

An STM image of a single CoTPP molecule is presented in Fig. 1a, together with a model highlighting the distortion of the macrocycle, which significantly differs from the structure of the molecule in three-dimensional crystallites, in which there are only minor ruffling distortions of the porphinato skeleton[19]. The saddle-shape conformation of the CoTPP macrocycle is similar on both Ag(111) and Cu(111) substrates, with pairs of opposite pyrrole rings tilted upwards (ανω-pyrrole, or α-pyr) or downwards (κατω-pyrrole, or κ-pyr) by an angle ρ of 20–30° (refs 11,12). Moreover, the phenyl substituents are rotated by the dihedral angle ($\theta \approx 45°$) out of the surface plane. The bending of opposing pyrrole groups leads to a characteristic imaging of the macrocycle as a triple protrusion when occupied states are probed[11,12,20]. Its core part reflects the metal centre, which is flanked by the two α-pyr moieties.

On Ag(111), CoTPP forms regular arrays (Fig. 1b). For the carbonyl attachment we exposed the sample to CO background pressures *in situ*. Following dosing with small amounts of CO, the array structure remained unaffected and the intramolecular features were still clearly resolved (this holds for the entire low-coverage regime

[1]Physik Department E20, TU München, James-Franck Strasse, D-85748 Garching, Germany, [2]Université de Lyon, Laboratoire de Chimie, ENS de Lyon, 46 allée d'Italie, 69364 Lyon cedex 07, France, [3]Department of Physics and Astronomy, University of British Columbia, Vancouver, British Columbia, Canada V6T1Z4, [4]Centre d' Investigació en Nanociència i Nanotecnologia (CSIC-ICN), Campus de la UAB, Bellaterra E-08193, Spain. *e-mail: jvb@ph.tum.de

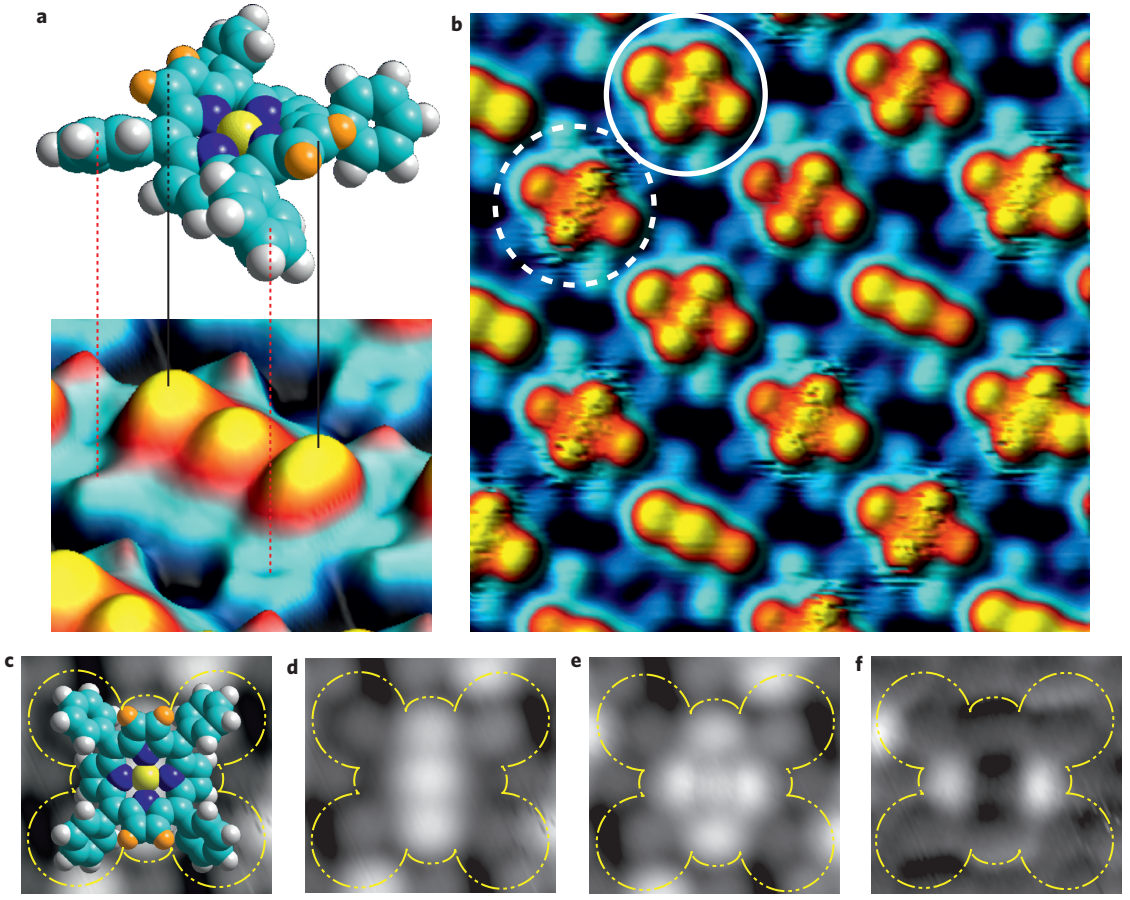

Figure 1 | Saddle-shape conformation of CoTPP on Ag(111) and response towards CO exposure. a, Conformational adaptation of CoTPP adsorbed on the (111) surfaces of copper or silver. The pseudo three-dimensional rendering of a high-resolution STM image shows the saddle-shaped macrocycle distortion and alternately rotated phenyl groups ($V = -0.7$ V, $I = 0.46$ nA). Pyrrole hydrogens pointing away from the surface (α-pyr moiety) are emphasized in orange. **b**, CoTPP array on Ag(111) following exposure to a small dosage of CO. There is a mixed layer comprising CoTPP, CO/CoTPP (dashed circle) and $(CO)_2$/CoTPP (solid circle). **c**, Top-view model of CoTPP overlaid on an STM image. **d**,**e**, Top-view topography of undecorated CoTPP (**d**) and dicarbonyl (**e**) species. **f**, The corresponding difference image emphasizes the ~5.3 Å between CO-related maxima.

investigated, as shown in the data series included in the Supplementary Information). However, a fraction of the CoTPP was decorated by two additional protrusions, located on either side of the Co centre, at the κ-pyr groups. Selective uptake of CO adducts has therefore occurred, resulting in a cross-like appearance of the porphyrin macrocycle. A closer inspection of Fig. 1b reveals that two similar CO-induced configurations are present. The first species (solid circle) shows five distinct protrusions and represents a stable entity, called a static cross. The second structure is topographically similar, but the CO-related features are imaged scraggy (dashed circle in Fig. 1b), which is an indication of rapid fluctuations with a frequency exceeding that used in the measurement. This is called a labile cross.

We unambiguously clarified the nature of the two distinct cross-shaped species by molecular manipulation experiments, using the STM tip as a tool to translate adsorbates across a surface, as has been successfully demonstrated for CO molecules at metal substrates[21–23]. We first positioned the tip above a static cross (stabilized at 500 mV and 30 pA; Fig. 2a,d) and lowered the tip towards the surface by increasing the current to 1 nA. Subsequently, the tip was laterally moved to an adjacent CoTPP molecule and finally retracted to its initial height. The following STM image shows that this procedure converts one static cross into two labile crosses (Fig. 2b,e). Applying the same procedure again, it is possible to reunite the two unstable species as one static cross, now localized at the neighbouring molecule (Fig. 2c,f). Single CO-related features can also be abstracted and irreversibly desorbed by applying higher voltage pulses. The static configuration must therefore be composed of two CO molecules attached to a single CoTPP, and represents a *cis*-dicarbonyl species. Accordingly, the labile cross is a related monocarbonyl complex. The protrusions associated with the CO adducts (Fig. 1c–f) occupy distinct, symmetric positions at the macrocycle κ-pyr moieties, the effect of which must be related to the porphyrin conformation. When there is only one CO attached, the carbonyl ligand rapidly flips between two equivalent sites, indicating that the corresponding energy barrier is rather low. Consequently, the effects of the proximity of the STM tip on flipping cannot be excluded. The slight asymmetry of the flipping carbonyl ligands imaged in Fig. 2e is therefore ascribed to tip–sample interactions; however, it was not possible to maintain the CO at a specific location in the manipulation experiments.

The unusual carbonyl ligation is not limited to the CoTPP/Ag(111) system. It appears in a similar manner with iron centres, as demonstrated by the STM image in Fig. 3a. For this experiment, we synthesized FeTPP directly on the Ag(111) surface by direct metallation of the macrocycle[20]. The generated FeTPP array was exposed to CO following the same experimental protocols as used for CoTPP. Additional *in situ* dosing with CO led to features with characteristics similar to those described above (Fig. 3a). Both static and labile crosses, corresponding to CO/FeTPP and $(CO)_2$/FeTPP, can be observed. The same procedures were also conducted with a different underlying metal surface, Cu(111), which

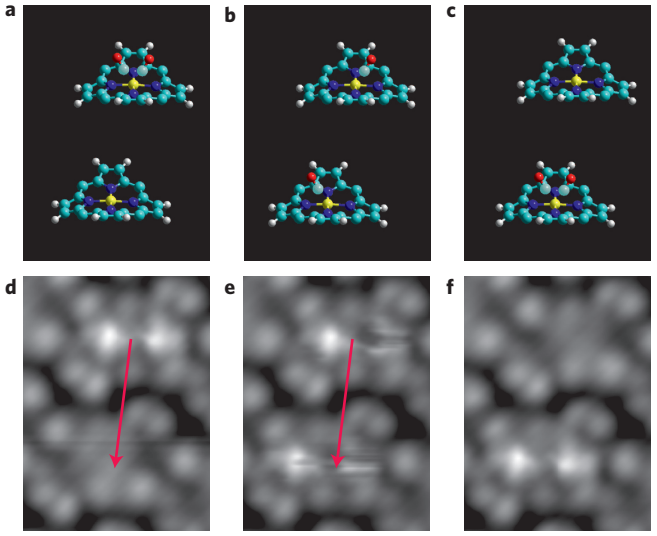

Figure 2 | Transfer of carbonyl ligands by molecular manipulation. **a–c**, Schematic model of two saddle-shaped porphyrin macrocycles with different ligation modes of two CO molecules (meso-phenyl groups are omitted for clarity) corresponding to the data sequence shown in the lower panel. **d–f**, STM images of CoTPP at a sample bias of 500 mV, demonstrating the sequential transfer of two CO adducts. The lateral manipulation steps are marked by red arrows and indicate the route of the STM tip converting a pristine CoTPP first to CO/CoTPP and subsequently to $(CO)_2$/Co-TPP.

has a smaller lattice parameter and higher chemical reactivity. Nevertheless, the characteristic MTPP–carbonyl features reappeared, as demonstrated in the STM image in Fig. 3b for the specific configuration of $(CO)_2$/CoTPP/Cu(111). In all cases, manipulation experiments could be successfully conducted to distinguish the respective carbonyl species.

These experimental findings allow us to conclude that the asymmetric monocarbonyl and symmetric *cis*-dicarbonyl attachment is potentially a universal feature of the saddle-shaped metallo-porphyrin conformers. Whereas dicarbonyl ligation in *cis*-geometry has been suggested for early transition-metal porphyrins, notably with Mo, it is definitely unexpected for Fe or Co centres[24,25]. The reason for this is the difference in electronic structure and atomic size, which results in sizable displacements for Mo centres out of the porphyrin plane, and therefore an eagerness to bind adducts in a multiple ligation mode. The present saddle-shape conformation could support a related ligation scheme; however, when we compare the STM topography of the observed species with dicarbonyl species generated at single adsorbed Fe or Co atoms, major differences appear. In particular, the distance between CO-related features in the present MTPPs significantly exceeds that in adatom dicarbonyls[22,26].

Theoretical analysis of CO adducts at saddle-shaped CoTPP

To rationalize the interplay between macrocycle conformation and CO ligation, we performed extensive DFT calculations. For surface-confined MTPP-carbonyls, we concentrate on the CoTPP/Cu(111) system. Before adding the ligand, the CoTPP is placed in the experimentally determined bridge position on Cu(111). The relaxed molecule displays significant bonding with the metal substrate. Interestingly, the connecting (or chemically bonded) areas are strongly localized due the non-planarity of the porphyrin molecule. There are three distinct locations: a strong Co–Cu bond (distance, 2.8 Å) and the di-σ bonding of two C=C bonds closest to the surface from the κ-pyr groups (C–Cu length, 2.2 Å). In the adsorbed state, cobalt porphyrin retains a saddle-shape

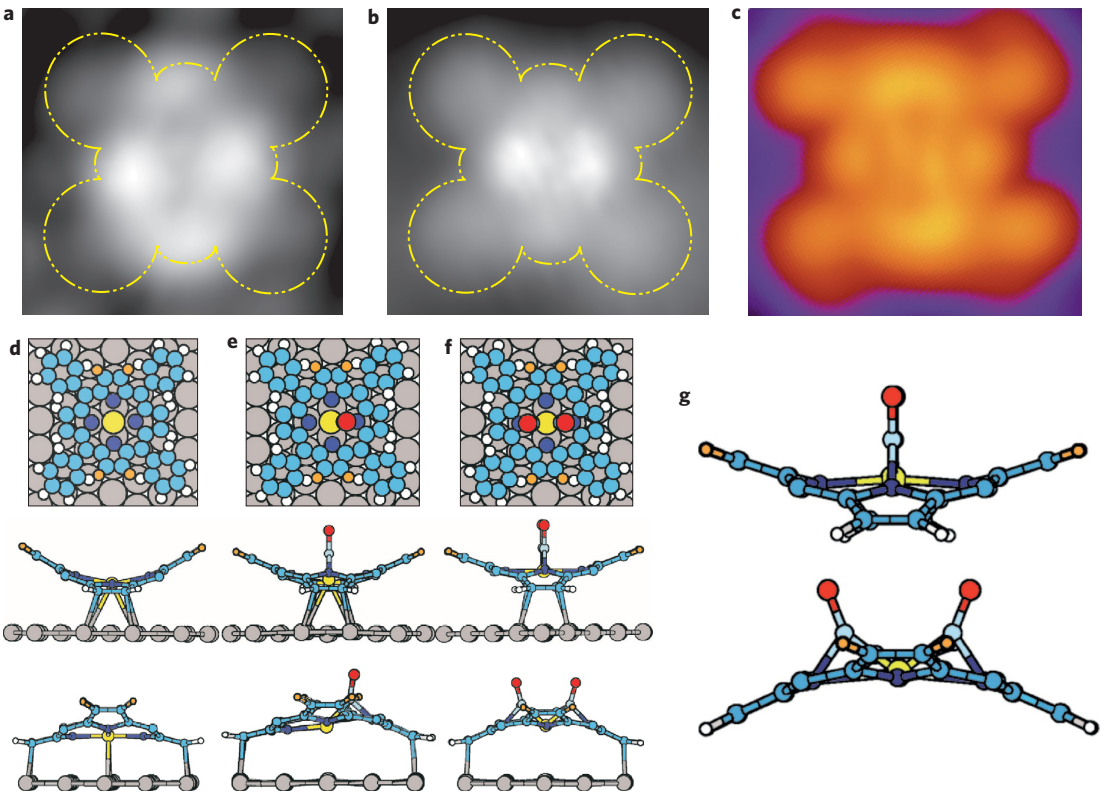

Figure 3 | Comparison of experimental data and theoretical description. **a**,**b**, STM images of $(CO)_2$/Fe-TPP on Ag(111) (**a**) and $(CO)_2$/Co-TPP on Cu(111) (**b**). **c**, Constant current simulation using the Tersoff-Hamman approximation at −0.6 V bias for $(CO)_2$/Co-TPP with two μ-carbonyl adducts on Cu(111) reproduces the main features of the experimental STM data. **d–f**, DFT modelling showing the relaxed geometry of the systems Co-TPP (**d**), CO/Co-TPP (**e**) and $(CO)_2$/Co-TPP (**f**) on Cu(111) with bridging μCO ligation. **g**, DFT model of stable, free $(CO)_2$/Co-TPP species in a *cis*-μ-dicarbonyl binding geometry.

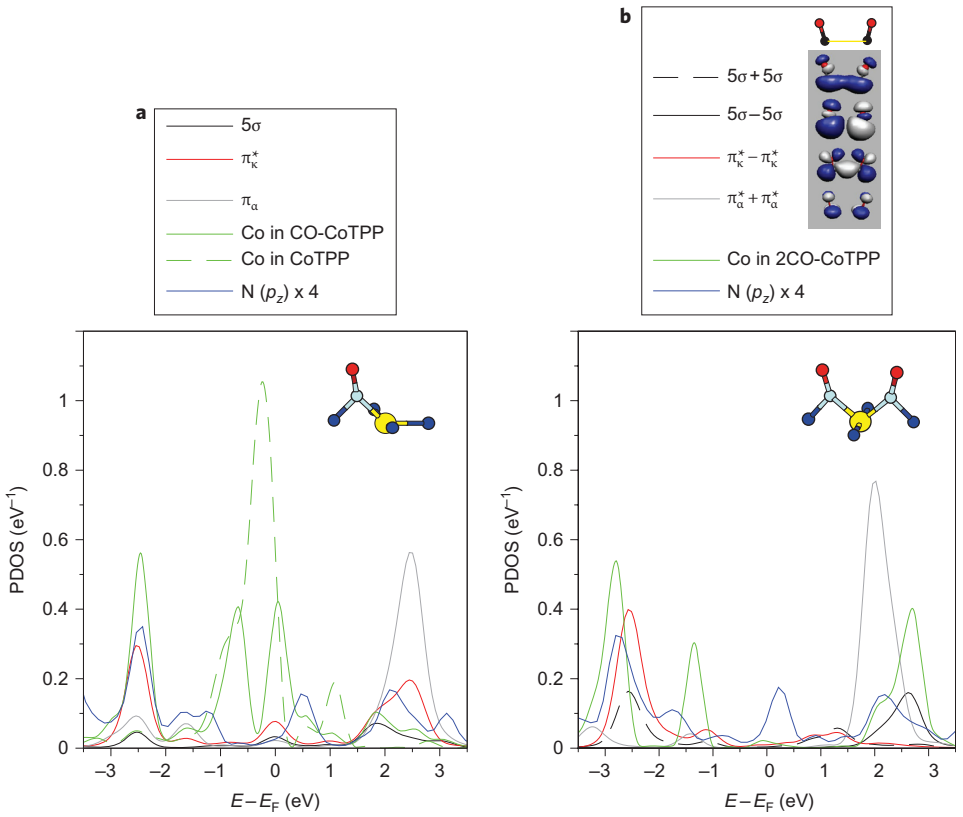

Figure 4 | Electronic properties of the bridged carbonyl complexes. a,**b**, PDOS of CO/Co-TPP (**a**) and $(CO)_2$/Co-TPP (**b**) adsorbed on Cu(111) onto the molecular states of the CO adducts and the active atomic states of Co and N atoms (d_{xz} Co and p_z N with z being the direction normal to the surface and x aligned with the Co-N_κ bond). The degenerate $2\pi^*$ states along the N_α and N_κ pyrrole subunits are indicated. The dimer molecular states are sketched and labelled with the combination of monomer states.

conformation. We considered several binding geometries for the carbonyl adducts, and the results definitely exclude a *cis*-dicarbonyl ligation at the metal centre. However, we found that the bending of the macrocycle yields a different option: a carbonyl ligand (μCO) that bridges the coordination bond between the iminic (–C=N–) nitrogen and metal centre. This ligand insertion scheme is favoured exclusively at the κ-pyr groups, both for steric reasons and because of the weaker dative Co–N_κ bonds. Thus, the bridging position allows the binding of two CO adducts at two opposed and equivalent sites of the porphyrin molecule. The corresponding STM image simulation for the dicarbonyl species (Fig. 3c) reproduces the main characteristics of the experimental topography, nicely rendering the carbonyl-related features.

With the μ-carbonyl ligand bonded to the macrocycle, the Co porphyrin adsorption structure is modified in two concomitant ways (Fig. 3d–f): vertical lifting of the central Co atom and rupture of the coupling with the metal substrate. However, it can readily be seen that the saddle-shape geometry is conserved overall. For one CO bridging ligand the effect is subtle and localized to the central cation: Co undergoes a small vertical shift towards the CO, weakening its bonding to the substrate, but the κ-pyr subunits remain anchored to the substrate. Here, calculations (Fig. 3, phenyl substituents not shown) reveal a sizeable stretching of the Co–N distance to 2.2 Å, under the carbonyl ligand. Following attachment of two carbonyls, a symmetrical adsorption structure is achieved, with the central cation detached from the surface (the Co–Cu distance increases to 3.5 Å), whereas the κ-pyr groups remain linked to the surface through a pronounced tilt of the pyrrole plane. A somewhat related behaviour occurs with NO ligation to CoTPP adsorbed on Ag(111), where the system response also includes suppression of the Co–substrate interaction[27]. With the present system, this strongly signals that the underlying surface is not directly determining the CO ligation mode; that is, it is not a result of a surface coordination architecture[28].

The novel complexation of two CO entities is also relevant to the gas-phase environment, as predicted by the DFT structure of the free complex (Fig. 3g). Subtle changes can be observed on the C atoms of the κ-pyr groups switching from sp^3 hybridization for the adsorbed species to sp^2 for the isolated species. Note that for isolated species in the saddle-shaped geometry, the bonding of carbonyl moieties on both opposite sides of the macrocycle plane cannot be excluded.

Formation of the carbonyl bridging complex is possible thanks to the chemical interaction between the two carbonyl ligands mediated by the Co centre. The two carbonyl ligands can be considered as a dimer entity linked through the cobalt centre, as outlined in the orbital diagram of Fig. 4. The plot shows the calculated density of states (DOS) projected onto the molecular states of the ligands for one (Fig. 4a) and two (Fig. 4b) bridging carbonyls, respectively. The CO frontier orbitals are the 5σ (HOMO) and degenerate $2\pi^*$ states (LUMO). On the bridging site on the molecule, the $2\pi^*$ states split and we mark them as $2\pi^*_\alpha$ and $2\pi^*_\kappa$ depending on whether they point to the N_α or N_κ pyrrole. The molecular resonances of the 5σ (HOMO, solid black line, Fig. 4a) and $2\pi^*_\kappa$ (LUMO, solid red line, Fig. 4a) states are further shifted and broadened in energy due to their strong orbital overlap with the corresponding pair of Co and N atoms of the adsorbed porphyrin molecule. Such energy shifting and broadening implies that the 5σ level becomes partially empty and the $2\pi^*_\kappa$ partially occupied, corresponding to the donation–back-donation bonding mechanism. For two CO ligands, the molecular states outlined in Fig. 4b (right) resemble those of a molecular dimer exhibiting a reduced

HOMO–LUMO gap compared to the monomer case, thus reinforcing bonding to the cobalt porphyrin. The antibonding combination of the 5σ (solid black line) and the bonding combination of the $2\pi^*_\kappa$ (solid red line), acting as HOMO and LUMO states of the $(CO)_2$ dimer, remain localized states but are respectively up- and downshifted relative to the Fermi level as a result of a complete donation and back-donation stabilizing the dimer on the porphyrin molecule.

Figure 4 also shows the projected DOS (PDOS) onto characteristic *d* Co and *p* N atomic orbitals. Without ligation of CO molecules by CoTPP, the Co d_{xz} PDOS is largely occupied (green dashed line). As one CO molecule is added, the d_{xz} orbital (green line in left panel of Fig. 4a) mainly rehybridizes with the 5σ and 2π of the bonded molecule, giving rise to common peaks coincidental in energy at –2.5 and +2.5 eV with respect to the Fermi level. These peaks agree well with the classical image of CO charge donation and back-donation (see Supplementary Information for further details; note that the d_{yz} orbital is much less affected, as expected from the binding geometry). The same is true for the peaks in the PDOS of the p_z orbital of the closest nitrogen atom. A second CO molecule leads to stronger rehybridization of the Co electronic structure, marked by the enhanced unoccupied *d* peak at +2.5 eV, while keeping the N-based electronic structure basically unchanged with respect to the mono-carbonyl case.

The calculated PDOS onto the Co *d* manifold completed by a Mulliken-like charge analysis provide relevant information on the charge state of the adsorbed Co atom before and after successive CO ligation (see Supplementary Information). It can be inferred that the Co(II) state of free CoTPP reduces to a Co(I) state following adsorption on Cu(111) due to the coupling between Co *d*-states and the Cu substrate. The adsorbed molecule is therefore in a non-magnetic singlet spin state.

The monocarbonyl ligation does not change the oxidation state of adsorbed Co, although the electronic structure is modified, rendering a doublet spin state. In contrast, the *cis*-dicarbonyl ligation again quenches the spin as a result of larger charge donation. The electronic characteristics of the adsorbed $CoTPP(CO)_2$ species are consistent with a Co(0) oxidation state.

We also performed a set of preliminary model calculations for the case of Fe centres, which indicated differences when compared to the results described above, but also signalled the possibility of bridged ligation. Note that the case for iron porphyrins is more diffcult to handle because of the higher complexity of modelling and experimental assessment of the Fe centre. Furthermore, a comparative assessment with the ligation of NO revealed that the expected conventional axial monocoordination pathway prevails, which is in perfect agreement with a recent study using space-averaging methods[27]. These results will be presented in full detail elsewhere.

Conclusions

We have identified a unique ligation mode for CO adducts at surface-supported cobalt and iron porphyrins by combined molecular-level STM observations and theoretical modelling. Notably, the saddle-shape conformation of both Fe– and Co–tetraphenylporphyrins induces a *cis*-carbonyl geometry, with CO binding to two spatially distinguished sites. Detailed calculations with Co centres reveal that CO bridges specific pyrrole groups with the metal atom, either as asymmetric monocarbonyl or symmetric *cis*-dicarbonyl species. This bonding scheme for CO adducts may be of general relevance regarding the chemical nature and functional behaviour of porphyrins with late transition-metal centres in situations where conformational distortions interfere.

Methods

The experiments were performed using a custom-designed STM housing a commercial low-temperature-STM (for details see www.lt-stm.com and ref. 23). The system base pressure was below 2×10^{-10} mbar, and all measurements were performed at 6 K to achieve high-stability and high-resolution topographic images. The Ag(111) and Cu(111) substrates were prepared using standard procedures (cycles of Ar^+ sputtering and annealing) to obtain extended flat terraces separated by monatomic steps. The etched tungsten tip was prepared by argon bombardment and silver- or copper-coated by controlled dipping into the bare surface. All STM images were taken in constant-current mode and treated using the WSxM program (www.nanotec.es). Molecules were deposited by organic molecular beam epitaxy (OMBE) from a quartz crucible held at 625 K for Co-TPP and 575 K for 2H-TPP with a typical rate below one monolayer per hour and at a background pressure in the range of 1×10^{-10} mbar. Fe-TPP was synthesized *in situ* by exposing a H2-TPP submonolayer to an atomic beam of Fe (purity 99.998%). Because the additional attachment of CO (purity 99.97%) was not possible at elevated temperatures, the sample was exposed to CO doses directly in the measurement position at $T = 6$ K, increasing to ~20 K during dosing.

Density functional theory. Calculations were carried out using the projected augmented wave (PAW) method within the local density approximation (LDA) as implemented in the VASP code[29]. We used a 400 eV energy cutoff and spin polarization. The periodic slab calculations were Γ-point only for a $11 \times 5\sqrt{3}$ unit cell, accounting for the diluted phase of porphyrins (approximately the single molecule limit). The Cu slab was modelled by three atomic monolayers, and the vacuum space between adjacent slabs corresponded to eight atomic monolayers. The surface Cu layer and all adsorbate atoms were relaxed until atomic forces were smaller than 0.05 eV per Å.

The molecule–surface interaction for this large π-orbital system is probably driven by van der Waals interactions, especially in the ligated case when the chemical contact between the metallic centre and the metallic substrate is disrupted. Popular exchange-correlation functionals suffer from their lack of non-local correlation terms including the dispersion energy. Here, we use LDA as a partially satisfactory solution for large-scale adsorption systems, for which further improvements (such as adding the dispersive interactions in a self-consistent way) are not yet feasible[30]. Calculations in LDA have yielded good results regarding the adsorption of large π-orbital molecular systems, thanks to an approximate compensation for the lack of van der Waals interactions by the LDA tending to overestimate binding energies[12,31–34].

Received 19 March 2010; accepted 25 November 2010; published online 9 January 2011

References

1. Spiro, T. G. & Kozlowski, P. M. Is the CO Adduct of myoglobin bent, and does it matter? *Acc. Chem. Res.* **34,** 137–144 (2001).
2. Collman, J. P., Boulatov, R., Sunderland, C. J. & Fu., L. Functional analogues of cytochrome *c* oxidase, myoglobin, and hemoglobin. *Chem. Rev.* **104,** 561–588 (2004).
3. Ghosh, A. Metalloporphyrin–NO bonding: building bridges with organometallic chemistry. *Acc. Chem. Res.* **38,** 943–954 (2005).
4. Hoard, J. L. Stereochemistry of hemes and other metalloporphyrins. *Science* **174,** 1295–1302 (1971).
5. Kratky, C. *et al.* The saddle conformation of hydroporphinoid nickel(II) complexes: structure, origin, and stereochemical consequences. *Helv. Chim. Act.* **68,** 1312–1327 (1985).
6. Barkigia, K. M., Chantranupong, L., Smith, K. M. & Fajer, J. Structural and theoretical models of photosynthetic chromophores. Implications for redox, light absorption properties and vectorial electron flow. *J. Am. Chem. Soc.* **110,** 7566–7567 (1988).
7. Barkigia, K. M. *et al.* Nonplanar porphyrins. X-ray structures of (2,3,7,8,12,13,17,18-octaethyl- and -octamethyl-5,10,15,20-tetraphenylporphinato)zinc(II). *J. Am. Chem. Soc.* **112,** 8851–8857 (1990).
8. Sparks, L. D. *et al.* Metal dependence of the nonplanar distortion of octaalkyltetraphenylporphyrins. *J. Am. Chem. Soc.* **115,** 581–592 (1993).
9. Shelnutt, J. A. *et al.* Nonplanar porphyrins and their significance in proteins. *Chem. Soc. Rev.* **27,** 31–41 (1998).
10. Senge, M. O. Exercises in molecular gymnastics—bending, stretching and twisting. *Chem. Commun.* 243–256 (2006).
11. Weber-Bargioni, A. *et al.* Visualizing the frontier orbitals of a conformationally adapted metalloporphyrin. *ChemPhysChem* **9,** 89–94 (2008).
12. Auwärter, W. *et al.* Site-specific electronic and geometric interface structure of Co-tetraphenyl-porphyrin layers on Ag(111). *Phys. Rev. B* **81,** 245403 (2010).
13. Springer, B. A., Sligar, S. G., Olson, J. S. & Phillips, G. N. Jr. Mechanisms of ligand recognition in myoglobin. *Chem. Rev.* **94,** 699–714 (1994).
14. Aono, S. Biochemical and biophysical properties of the CO-sensing transcriptional activator CooA. *Acc. Chem. Res.* **36,** 825–831 (2003).
15. Kim, H. P., Ryter, S. W. & Choi, A. M. K. CO as a cellular signaling molecule. *Annu. Rev. Pharmacol. Toxicol.* **46,** 411–449 (2006).
16. Kachalova, G. S., Popov, A. N. & Bartunik, H. D. A steric mechanism for inhibition of CO binding to heme proteins. *Science* **284,** 473–476 (1999).
17. Sigfridsson, E. & Ryde, U. On the significance of hydrogen bonds for the discrimination between CO and O_2 by myoglobin. *J. Biol. Inorg. Chem.* **4,** 99–110 (1999).

18. Leu, B. M. *et al.* Quantitative vibrational dynamics of iron in carbonyl porphyrins. *Biophys. J.* **92,** 3764–3783 (2007).
19. Madura, P. & Scheidt, W. R. Stereochemistry of low-spin cobalt porphyrins. 8. α,β,γ,δ-Tetraphenylporphinatocobalt(II). *Inorg. Chem.* **15,** 3182–3184 (1976).
20. Auwärter, W. *et al.* Controlled metalation of self-assembled porphyrin nanoarrays in two dimensions. *ChemPhysChem* **8,** 250–254 (2007).
21. Meyer, G., Neu, B. & Rieder, K. H. Controlled lateral manipulaiton of single molecules with the scanning tunneling microscope. *Appl. Phys. A* **60,** 343–345 (1995).
22. Lee, H. J. & Ho, W. Single-bond formation and characterization with a scanning tunneling microscope. *Science* **286,** 1719–1722 (1999).
23. Auwärter, W. *et al.* Molecular nanoscience and engineering on surfaces. *Int. J. Nanotechnol.* **5,** 1171–1193 (2008).
24. Brand, H. & Arnold, J. Recent developments in the chemistry of early transition metal porphyrin compounds. *Coord. Chem. Rev.* **140,** 137–168 (1995).
25. Smith, P. D., James, B. R. & Dolphin, D. H. Structural aspects and coordination chemistry of metal porphyrin complexes with emphasis on axial ligand binding to carbon donors and mono- and diatomic nitrogen and oxygen donors. *Coord. Chem. Rev.* **39,** 31–75 (1981).
26. Wahl, P. *et al.* Kondo effect of molecular complexes at surfaces: ligand control of the local spin coupling. *Phys. Rev. Lett.* **95,** 166601 (2005).
27. Flechtner, K., Kretschmann, A., Steinrück, H. P. & Gottfried, J. M. NO-induced reversible switching of the electronic interaction between a porphyrin-coordinated cobalt ion and a silver surface. *J. Am. Chem. Soc.* **129,** 12110–12111 (2007).
28. Barth, J. V. Fresh perspectives for surface coordination chemistry. *Surf. Sci.* **603,** 1533–1541 (2009).
29. Kresse, G. & Joubert, D. From ultrasoft pseudopotentials to the projector augmented-wave method. *Phys. Rev. B* **59,** 1758–1775 (1999).
30. Mercurio, G. *et al.* Structure and energetics of azobenzene on Ag(111): benchmarking semiempirical dispersion correction approaches. *Phys. Rev. Lett.* **104,** 036102 (2010).
31. Vladimirova, M. *et al.* Substrate-induced supramolecular ordering of functional molecules: theoretical modelling and STM investigation of the PEBA/Ag(111) system. *Acta Mater.* **52,** 1589–1596 (2004).
32. Rohlfing, M., Temirov, R. & Tautz, F. S. Adsorption structure and scanning tunneling data of a prototype organic–inorganic interface: PTCDA on Ag(111). *Phys. Rev. B* **76,** 115421 (2007).
33. Klappenberger, F. *et al.* Conformational adaptation in supramolecular assembly on surfaces. *ChemPhysChem* **8,** 1782–1786 (2007).
34. Franke, K. J. *et al.* Reducing the molecule–substrate coupling in C_{60}-based nanostructures by molecular interactions. *Phys. Rev. Lett.* **100,** 036807 (2008).

Acknowledgements

This work was supported by the European Research Council Advanced Grant MolArt (no. 247299), the Deutsche Forschungsgemeinschaft Cluster of Excellence Munich Center for Advanced Photonics, Canadian National Science and Engineering Research Council (NSERC) and Canada Foundation for Innovation (CFI). W.A., A.W.-B. and J.R. thank the Technische Universität München Institute for Advanced Studies, the German Academic Exchange Service and the Deutsche Forschungsgesellschaft for scholarships, respectively. M.–L.B. acknowledges computational time at the Leibniz Rechenzentrum Garching. N.L. thanks Spanish Ministerio de Ciencia e Innovación for financial support (grant no. FIS2009-1271-C04-01).

Author contributions

K.S., W.A., A.W.-B. and J.R. performed the STM experiments, and analysed and interpreted the experimental data. The theoretical analysis was provided by M.-L.B. and N.L. J.V.B., W.A. and M.-L.B. conceived the studies and co-wrote the paper with K.S. and N.L.

Additional information

The authors declare no competing financial interests. Supplementary information accompanies this paper at www.nature.com/naturechemistry. Reprints and permission information is available online at http://npg.nature.com/reprintsandpermissions/. Correspondence and requests for materials should be addressed to J.V.B.